Journal of Pharmaceutical Investigation
DOI 10.1007/s40005-014-0151-2

RESEARCH ARTICLE

Angiopep-2-conjugated liposomes encapsulating γ-secretase inhibitor for targeting glioblastoma stem cells

Shuhua Xuan · Dae Hwan Shin · Jin-Seok Kim

Received: 16 July 2014 / Accepted: 24 August 2014

Abstract $CD133^+$ cell subpopulation in U87 MG cells displays glioblastoma stem cell (GSC) like properties. Notch, a key regulator of stem cells, is also over-activated in GSCs. It was previously reported that γ-secretase inhibitors inhibit the Notch pathway by targeting the γ-secretase complex. To examine the GSCs, $CD133^+$ cells were separated from the U87 MG cells by magnetic activated cell sorting and only cell populations with nearly 90 % $CD133^+$ cells were used as GSCs. The sorted U87-$CD133^+$ cells indeed display enhanced chemoresistance and high Notch activity. For targeting studies, Angiopep-2 (An2)-conjugated YO-01027 (YO) encapsulating liposomes (PEG-lipo-YO-An2) were prepared by lipid film hydration method. An2 is an effective ligand of low density lipoprotein receptor-related protein which is over-expressed in the blood–brain barrier and GSCs. The mean diameter, zeta potential and encapsulation efficiency of PEG-lipo-YO-An2 was around 180 nm, −10.0 mV and 56.6 %, respectively. In in vitro studies, we confirmed that PEG-lipo-YO-An2 showed enhanced anti-GSC properties such as enhanced stability, anti-proliferation and anti-tumor sphere formation abilities towards than free drug. This study demonstrates that An2 conjugation and liposomal encapsulation of YO enhance the cytotoxicity of YO against GSCs, and this formulation could be used as a promising candidate for the treatment of glioblastoma multiforme by targeting GSCs.

Shuhua Xuan and Dae Hwan Shin equally contributed as first-authors to this study.

S. Xuan · D. H. Shin · J.-S. Kim (✉)
Research Center for Cell Fate Control (RCCFC) & College of Pharmacy, Sookmyung Women's University, Chungpa-Dong 2-Ga, Youngsan-Gu, Seoul, Korea
e-mail: jsk9574@sm.ac.kr

Keywords γ-Secretase inhibitor · CD133 · Angiopep-2 · Glioblastoma multiforme · Liposome

Introduction

Glioblastoma multiforme (GBM) is the most common malignant tumor of the central nervous system, it is also a devastating brain tumor with an average survival time from the initial diagnosis of about 1 year (Maher et al. 2001; Ohgaki and Kleihues 2005; Wen and Kesari 2008). Despite modern advances in surgery, radiation and chemotherapy, treatment of GBM is often palliative and gradually results in therapy-resistance (Hu et al. 2011). Recently, a small subpopulation of stem cell-like properties is thought to be critical for the engraftment and long-term propagation of malignant tumors, including GBM (Reya et al. 2001; Singh et al. 2004; Sanai et al. 2005). This subpopulation of GBM cells have been referred to as glioblastoma stem cells (GSCs) (Park and Rich 2009). There is an accumulating evidence that GSCs with potential for self-renewal and multi-lineage differentiation, plays an important role in glioma initiation, growth, and recurrence (Hemmati et al. 2003; Galli et al. 2004; Singh et al. 2004; Yuan et al. 2004). CD133, also known as prominin-1 (PROM-1), is transmembrane glycoprotein family member which expressed as several isoforms with unknown physiological or pathological function (Miraglia et al. 1997; Yu et al. 2002; Singh et al. 2004). GSCs have been prospectively enriched by selection of the CD133 cell surface marker, and only $CD133^+$ cells from brain tumor biopsy specimens were capable of initiating brain tumor in an immunodeficient mouse model (Hemmati et al. 2003; Singh et al. 2003, 2004).

Published online: 03 September 2014

A number of signal pathways are involved in the formation and maintenance of stem cells, including the Notch signaling pathway. Notch signaling is a well-conserved cell–cell communication that plays a pivotal role in the maintenance of neural stem cells (NSCs) (Louvi and Artavanis-Tsakonas 2006; Wang et al. 2010; Hu et al. 2011). Aberrant Notch signaling and mutations in the components of the pathway contributed to cancer formation have been gradually established T cell leukemia (T-ALL) and various cancers including in breast, colon, prostate, melanoma (Radtke and Raj 2003; Rizzo et al. 2008). Moreover, many studies have implicated a role for Notch signaling in GSCs (Fan et al. 2006; Hu et al. 2011, 2014; Garner et al. 2013; Guichet et al. 2014; Saito et al. 2014). Notch signaling is initiated when transmembrane ligands on one cell bind Notch receptors on a neighboring cell, the γ-secretase-mediated sequential proteolytic cleavages that eventually lead to release of the Notch intracellular domain (NICD), then the NICD translocates into the nucleus where it interacts with transcriptional cofactor (CBF1) leading to activation of target genes such as the Hey, Hes and c-Myc genes, which are associated with cell proliferation, differentiation and apoptosis (Iso et al. 2003; Ehebauer et al. 2006). Furthermore, Notch also plays a significant role in tumor angiogenesis, which is essential for tumor growth and metastasis (Ridgway et al. 2006; Li et al. 2007). Thus, Notch is a promising target for cancer treatment. Several preclinical and clinical studies have been launched to test efficacy and safety of Notch inhibitors in cancer therapy (Sahebjam et al. 2013; Schott et al. 2013). Inhibition of Notch signaling directly caused cell cycle exit, apoptosis, differentiation, and impaired tumorigenic capacity of the CD133-positive cells in GBM cells, while increased Notch activity enhances Nestin expression, promotes the cell proliferation, survival and the formation of NSC-like colonies and plays an important role in the brain tumor stem cells (Shih and Holland 2006; Zhang et al. 2008; Hovinga et al. 2010). Despite the availability of efficient Notch inhibitors such as γ-secretase inhibitors (GSI), peptides (Moellering et al. 2009) or antibodies (Wu et al. 2010; Yan et al. 2010), the GSIs are the only form of Notch inhibitors in clinical trials (Purow 2012). GSIs were originally developed as potential therapies to treat Alzheimer's disease, as they block the γ-secretase complex, cleave the Aβ precursor protein (APP) to yield of Aβ peptides (Zhang et al. 2013). Recently GSIs have gained more attention as novel anti-cancer drugs due to their ability to block the Notch signaling pathway (Wang et al. 2008).

YO-01027 (YO), also known as dibenzazepine, is a dipeptidic GSI which blocks the Notch signaling pathway and inhibits epithelial cell proliferation and induces differentiation (van Es et al. 2005; Telerman and Amson 2009). However, due to the demand for Notch signaling in most of normal tissues, GSIs treatment give rise to potential risks including gastrointestinal toxicity and suppression of lymphopoiesis (Wong et al. 2004; van Es et al. 2005). So, Notch inhibition as cancer therapy may be problematic for their use in human due to their lack of specificity (Purow 2012). It is also hard to deliver the GSIs effectively to the GBM as well as infiltrating GSCs that are located in the tumor bed. Because the most GSIs are small and have poor water solubility, they require vehicles to be able to carry adequate amounts of hydrophobic drugs (Mamaeva et al. 2011). Therefore, more efficient targeted delivery system which specifically suppresses the Notch activity in GSCs is required.

Almost 100 % large-molecule drugs and more than 98 % small molecule candidate agents are unable to reach the brain tumor tissue due to their rare blood–brain barrier (BBB) penetration and poor glioma targeting (Pardridge 2005, 2007; Xin et al. 2012a). The permeability of the BBB is regulated by the brain capillary endothelial cells (BCECs) which are tightly connected by tight junctions (Pardridge 1999). It has been reported that a series of receptors are presented at the BBB, including the transferrin receptor, insulin receptor and low-density lipoproteins (Huang et al. 2011). Among them, the low density lipoprotein receptor-related protein (LRP) has been reported that it could mediate transport of ligands across endothelial cells of the BBB, and LRP1 is over-expressed on glial cells, compared with the normal tissue (Lopes et al. 1994). Angiopep-2 (An2), as a ligand of the LRP1 and one of the novel family peptides that derived from the Kunitz domain, exhibits a higher brain penetration capability than other proteins, transferring and aprotinin (Demeule et al. 2008). It is also reported that An2 modified drug delivery system possess an excellent ability to cross the BBB (Ren et al. 2012; Shao et al. 2012; Sun et al. 2012; Xin et al. 2012b). All these results highly demonstrate that An2 may be a potential ligand that can be used not only for enhanced delivery across the BBB but also for further targeting the glial cells. Therefore, take account into the advantage of dual-targeting using the same ligand, An2 was used as a potential targeting moiety in the present work.

It is well known that liposomes are spherical shape made from naturally-derived phospholipids, which are biocompatible carriers using in drug delivery system (Akbarzadeh et al. 2013). YO, as a hydrophobic drug, could be dissolved into the membrane of liposomes. And conjugation of polyethylene glycol (PEG) which is widely used as polymeric steric stabilizer, reduce degradation of liposomal formulation of YO in reticular endothelial system (RES) (Gref et al. 2000). Thus, PEGylation of liposome increase their blood circulation time and tumor accumulation after intravenous administration (Chow et al. 2009).

In this work, we have developed a therapeutic liposomal YO formulation against GSCs by targeting Notch activity. To overcome the rapid clearance by RES, the surface of liposomes were modified with flexible hydrophilic polymers such as PEG. And to establish a dual-targeting drug delivery, the PEGylated liposomes modified with An2. Then, YO loaded PEGylated liposomes modified with An2 (PEG-lipo-YO-An2) was evaluated for their physical characterization and in vitro study using GSCs.

Materials and methods

Materials

YO-01027 was purchased from Selleckchem (Houton, USA) and cysteine-An2 (TFFYGGSRGKRNNFKTEEYC, MW = 2,404.6) was synthesized by Peptron Inc. (Daejeon, Korea). L-α-phosphatidylcholine (EPC) and 1,2-distearoyl-sn-glycero-3-phosphoethanolamine-*N*-[maleimide(polyethylene glycol)-2000] (ammonium salt) (DSPE-PEG (2000) Maleimide) were purchased from Avanti Polar-Lipids Inc. (Alabaster, USA). The anti-CD133 monoclonal antibody and β-actin antibody were purchased from Abnova Co. (Taipei, Taiwan). Temozolomide (TMZ), trifluoroacetic acid, isopropanol, hexane–sulfonic acid sodium salt, 3-(4,5-dimethylthiaYO-2-yl)-2,5-diphenyl-2*H*-tetrazolium bromide (MTT), Methanol (MeOH), chloroform ($CHCl_3$), dimethyl sulfoxide (DMSO), accutase, human epidermal growth factor (hEGF), fibroblast growth factor-basic (bFGF), cholesterol (Chol) and Sephadex G-75 were purchased from Sigma Chemical Co. (St. Louis, USA). GIBCO® Dulbecco's Modified Eagle Medium: Nutrient Mixture F-12 (DMEM/F12) and B-27 supplement (B27) were purchased from CureBio (Seoul, Korea). Dulbecco's Modified Eagle's Medium (DMEM), fetal bovine serum (FBS), trypsin–EDTA, Dulbecco's phosphate-buffered saline (DPBS) and penicillin/streptomycin were purchased from Welgene Inc. (Daegu, Korea). BCA protein assay kit was purchased from Bio-Rad Laboratories, Inc. (Hercules, USA). Forward and reverse primers of Hey1, c-Myc and GAPDH were purchase from Bioneer Inc. (Daejeon, Korea). TRIYO® reagent was purchased from Invitrogen (Carlsbad, USA). RNA to cDNA EcoDry™ Premix (Oligo dT) was purchased from Takara Bio Inc. (Shiga, Japan). All reagents and solvents were of analytical grade or better.

Sorting of CD133 subpopulations by magnetic-activated cell sorting (MACS) technology

U87 MG, a human GBM cell line was purchased from the American Type Culture Collection (ATCC; Manassas, USA) and maintained as monolayer in DMEM containing 10 % FBS and antibiotics (100 U/ml penicillin, 100 U/ml streptomycin) at 37 °C in a humidified atmosphere of 5 % CO_2. In order to form neurospheres, U87 MG cells were cultivated in serum-free DMEM/F12 medium supplemented with hEGF (20 ng/ml), bFGF (20 ng/ml), B27 (1:50), and penicillin–streptomycin (100 U/ml). Neurospheres were collected after 7 days and disaggregated with accutase solution. The $CD133^+$ cells (GSCs) were separated by a MACS separation kit (Miltenyi Biotec Ltd., Teterow, Germany). Briefly, 1×10^8 cells per 300 µl MACS buffer (PBS, 2 mM EDTA, 0.5 % BSA) were incubated with 100 µl FcR blocking reagent and added 100 µl CD133 microbeads solution for 30 min on ice. Then, the $CD133^+$ and $CD133^-$ cells were separated using the magnetic column following the manufacturer's instructions. The efficiency of sorting was verified by fluorescence-activated cell sorting (FACS), Western blot, and quantitative real-time reverse transcription PCR (qRT-PCR) analysis. Cells containing nearly 90 % $CD133^+$ cell fraction were used as GSCs for experimentation.

Characterization of GSCs

To estimate the expression of GSC marker CD133 in the sorted cells ($CD133^+$ and $CD133^-$), FACS, Western blotting and qRT-PCR analysis were performed. The efficiency of sorting was verified by FACS, labeled with a phycoerythrin (PE)-conjugated-CD133/2 antibody (CD133-PE; Miltenyi). In Western blot analysis, cells were lysed by extracting proteins with lysis buffer (50 mM Tris–HCl pH 7.4, 150 mM NaCl, 0.1 % Triton X-100) supplemented with protease inhibitors on ice. Protein concentrations were determined with BCA protein assay kit. Proteins in each cell lysate are subjected to SDS-PAGE, and transferred onto PVDF membranes, then probed with primary CD133-Ab overnight at 4 °C, followed by horseradish peroxidase-labeled antibodies (Kierkegaard & Perry Laboratories, Inc., Gaithersburg, USA). CD133 band was detected by enhanced chemiluminescence (Supersignal® West pico chemiluminescent substrate; ThermoScientic, Rockford, USA) according to the manufacturer's protocol. β-actin antibody was used as the internal protein control. In separate experiment for analysis of Notch activity, the expression of Notch target gene (Hey1 and c-Myc) mRNA in sorted cells was determined by qRT-PCR. Briefly, total RNA in sorted cells was extracted using TRIYO® reagent according to the manufacture's protocol. The concentration and purity of isolated RNA were detected by NanoDrop spectrometer (Epoch; BioTeck, Arcugnano, Italy). cDNA synthesis was performed by PCR thermal cycler Dice (Takara, Shiga, Japan) using RNA to cDNA Ecodry™ (Takara). The synthesized cDNA was subjected to real time-PCR amplification with power SYBR® Green (Applied Biosystems,

Warrington, UK) using ABI PRISM 7500 sequence detector (Applied Biosystems). All samples were amplified in triplicates. The relative mRNA expression of Hey1 and c-Myc was normalized with GAPDH mRNA. Primer sequences are listed as follows:

Hey1 (forward):	ACGAGACCGGATCAATAACA
(reverse):	ATCCCAAACTCCGATAGTCC
c-Myc (forward):	GGA ACG AGC TAA AAC GGA GCT
(reverse):	GGC CTT TTC ATT GTT TTC CAA CT
GAPDH (forward):	AAC GTG TCA GTG GTG GAC CTG
(reverse):	AGT GGG TGT CGC TGT TGA AGT

Chemotherapeutic resistance of GSCs and non-GSCs cells

To compare the chemoresistance of sorted $CD133^+$ and $CD133^-$ cells, we tested TMZ, first-line treatment in primary GBM, using a MTT assay. The cells were seeded onto 96-well plates (3×10^3 cells per well) and treated with different concentrations of TMZ. After incubating for 48 h, the culture medium was removed and MTT solution (1 mg/ml) was added. The cells were incubated for 4 h, and then the medium was removed and replaced 100 µl DMSO to dissolve the formazan crystals. The absorbance of each well was measured at 570 nm wavelength using an ELISA reader (EL 800; BioTek, Winooski, USA). Measurements were made in triplicate, and values are presented as mean ± SD. The 50 % inhibitory concentration (IC_{50}) value was calculated using Sigmaplot version 10.0 software.

Preparation of PEGylated liposomes encapsulating YO

PEGylated liposomes were prepared with phospholipids and cholesterol by film hydration method. The 25 mM lipid mixture composed of EPC:Chol: DSPE-mPEG2000-maleimide (60:40:1 molar ratio) with 1 mg YO were dissolved in 1 ml of chloroform. The organic solvent was evaporated under nitrogen gas flow by a rotary evaporator (Laborota 4000, Heidolph, Italy) at room temperature. The dry lipid film was hydrated in 1 ml of PBS with vortexing and 30 s for sonication (Laboratory Supplies Co., Inc, NY, USA). The liposomes were downsized by extrusion through 0.45 and 0.2 µm cellulose membrane filter (Whatman Int. Ltd., Pittsburg, USA) for 5 times, respectively, using a Lipex™ extrusion device (Northern Lipids Inc., Vancouver, Canada). The unencapsulated YO was removed from liposomes suspension by gel chromatography using Sephadex G-75 column (Sigma).

Conjugation of An2 to liposomes

The PEGylated liposome-maleimide was conjugated with cysteine-An2 (1:1, mol/mol) and carried out in PBS for 24 h at a room temperature with stirring. The reacted mixture was dialyzed in distilled water at room temperature for 24 h to remove unconjugated cysteine-An2.

Size distribution and zeta potential analysis

The size distribution and zeta potential of liposomes were measured by dynamic laser-light scattering system (NICOMP 380ZLS, Inc., Santa Clara, USA) using a He–Ne laser light source. All measurements were performed at room temperature with 90° scattering angle.

Encapsulation efficiency of YO into liposomes

The concentration of YO in the liposomes was calculated by high performance liquid chromatography (HPLC). Briefly, 100 µl samples were diluted by adequate acetonitrile and mixed thoroughly on a vortex mixer. After centrifugation (13,300 rpm, 20 min), the acetonitrile extract was removed and the supernatant was evaporated under the nitrogen gas. The residue was resuspended in 100 µl of MeOH with vortexing, and 50 µl of sample was injected into the HPLC system. Conditions of HPLC system were shown in Table 1. Mobile phase was prepared with filtered and degassed acetonitrile and isopropanol (45:52) and its pH adjusted to 4.7 by addition of hexane–sulfonic acid sodium salt solution with 20 % trifluoroacetic acid. The amount of YO encapsulated in liposomes sample was determined from calibration curve of free YO. In encapsulation efficiency of YO (%) was calculated using the following formula;

$$\text{Encapsulation efficiency of YO } (\%) = \frac{\text{Amount of YO from liposomes}}{\text{Initial loading amount of YO in preparing process}} \times 100$$

Serum protein adsorption assay

The adsorption of serum proteins onto liposomes was evaluated by measuring the amount of bovine serum albumen (BSA) bound to liposomes in vitro. When liposomes are unstable and aggregated, the amount of protein adsorption will be increased. Briefly, non-PEGylated liposomes without the drug (non-PEG-lipo-empty), PEGylated liposomes without the drug (PEG-lipo-empty),

Table 1 HPLC analytical conditions for YO

Factors	Analytical conditions
Mobile phase	0.1 % hexane sulfonic acid (pH adjusted to 4.7 with 20 % trifluoroacetic acid), acetonitrile and isopropanol (45:52:3)
Flow rate	1.0 ml/min
Detector	UV/VIS detector (wavelength: 227 nm)
Column	Capcellpak® C18 (4.6 × 150 mm, 5 µm, SHISEIDO)
Injection volume	50 µl

PEGylated liposomes with YO (PEG-lipo-YO) and PEG-lipo-YO-An2 were incubated with 1 % (w/v) BSA dissolved in PBS (pH 7.4) at 37 °C. After incubation for 0.5, 3, 10, 24 and 48 h, samples were centrifuged at 14,000 rpm for 15 min. The free BSA in the supernatant was removed, and the liposomes were washed three times with PBS followed by centrifugation at 14,000 rpm for 15 min. The amount of proteins adsorbed onto the liposomes was measured with a BCA Protein Assay Kit using BSA as a standard. The absorbance was measured at 570 nm using an ELISA reader (BioTek).

In vitro anti-proliferation assay

GSCs which were dissociated and seeded onto 96-well tissue culture plates (3×10^3 cells/well) and incubated for 24 h at 37 °C, were treated with DPBS, 0.1 % DMSO, PEG-lipo-empty, Naked YO, PEG-lipo-YO and PEG-lipo-YO-An2 for 48 h. After incubation, cell growth was measured by MTT assay, as described above.

An2-mediated internalization was further supported by the competition assay (Mamaeva et al. 2011; Xin et al. 2011) with naked An2. An2 was added to the wells containing 3×10^3 of GSCs in advance at a concentration of 200 µg/ml. After 30 min incubation at 37 °C, the An2 medium was withdrawn from the wells and PEG-lipo-YO-An2 was treated. After 48 h incubation, cell growth was measured by MTT assay as described above.

Tumor spheres formation assay

GSCs were dissociated and seeded on 96-well plate (1–2 cells/well) with serum-free DMEM/F12 and incubated for 2 weeks to form tumor sphere (Shi et al. 2013). The wells containing only one sphere were treated with various YO formulations (10 µM). After 48 h incubation, the images of sphere colonies were observed using a light microscope (IX71IX51; Olympus, Tokyo, Japan).

Statistical analysis

Data are presented as a mean value ± standard deviation (SD). Statistical analyses were performed using Student's *t* test. Statistical significance was assigned for *P* values <0.05 (95 % confidence level) or <0.01 (99 % confidence level).

Results

Isolation and characterization of GSCs

It has been reported $CD133^+$ population in GBM was thought to be GSCs (Singh et al. 2003, 2004). GSCs can be cultured in suspension in serum-free medium with specific growth factors such as B27, bFGF and hEGF, generating neurospheres (Zhu et al. 2010). Under these special circumstances, expansion and growth of GSCs was improved (Yuan et al. 2004). The GSCs population in U87 MG cells was collected by disaggregating the neurospheres and separating the $CD133^+$ cells population using MACS technology employing CD133-Ab magnetic beads. As shown in Fig. 1a, CD133-Ab-sorted cells (GSCs) indeed formed spheroid bodies, exhibiting an ability to form neurospheres. As shown in Fig. 1b, the percentages of CD133-expressing cells determined by FACS analysis were 5.55 % in $CD133^-$ cells and 88.8 % in CD133-Ab sorted GSCs. Western blotting analysis also revealed that CD133 expression levels were significantly higher in GSCs than in $CD133^-$ cells (Fig. 1c). In chemoresistance experimentation, the IC_{50} values for TMZ were about 50 times higher in GSCs than $CD133^-$ cells (50 µM) (Fig. 2a). Thus, compared to $CD133^-$ cells, $CD133^+$ cells maintained a higher survival fraction and thereby possessed higher clinical chemoresistance. We also determined mRNA expression of Notch target gene by qRT-PCR, revealing that GSCs expressed higher Hey1 (Fig. 2b) and c-Myc (Fig. 2c) mRNA levels than $CD133^-$ cells.

Physicochemical characterization of liposomes

The liposomal formulation containing YO (Fig. 3a) used in this study is summarized in Table 2. The average diameter of non-PEG-lipo-empty, PEG-lipo-empty, PEG-lipo-YO and PEG-lipo-YO-An2 was approximately 197 ± 16, 185 ± 20, 189 ± 29 and 178 ± 29 nm, respectively. All of the liposomes tested maintained a negative zeta-potential (−6.93 to −10.09 mV).

The encapsulation efficiency of YO was measured by HPLC analysis, with the retention time being 4.73 min (Fig. 3b). The encapsulation efficiency of YO encapsulated

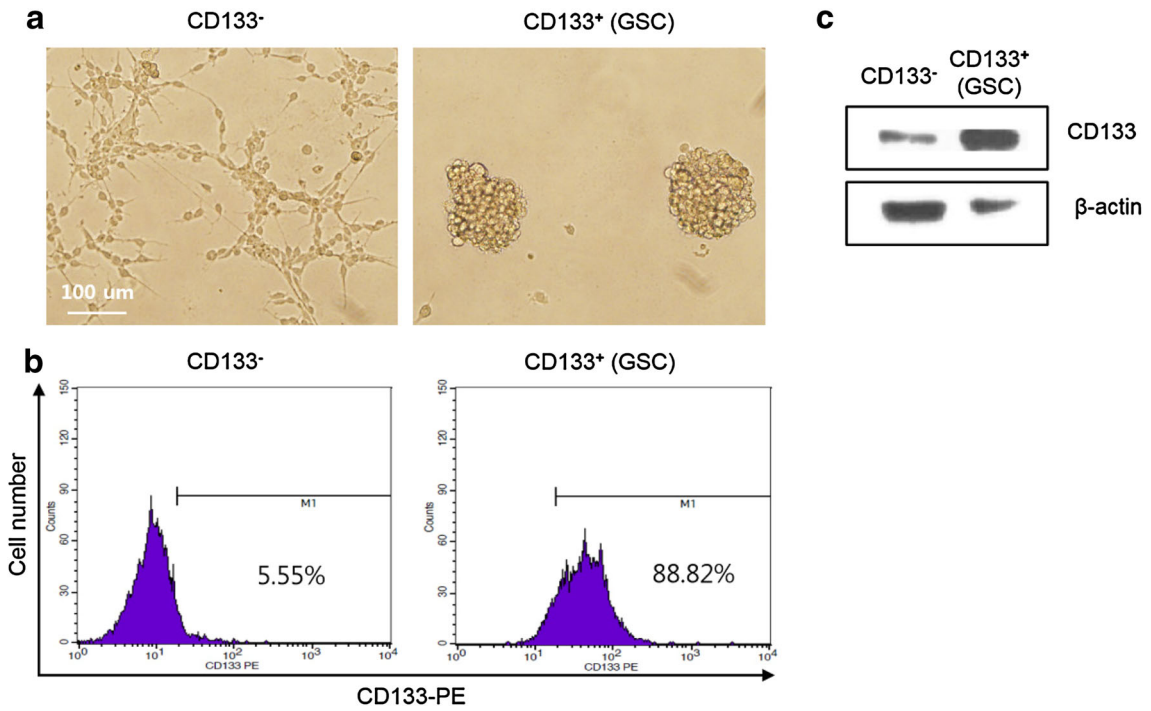

Fig. 1 Isolation and characterization of GSCs. **a** Images of $CD133^-$ cells and $CD133^+$ cells morphology after magnetic cell sorting under the light microscopy (*scale bar* 100 μm). CD133 expression in subpopulations of U87 MG cells analysis by FACS (**b**) and Western blotting (**c**)

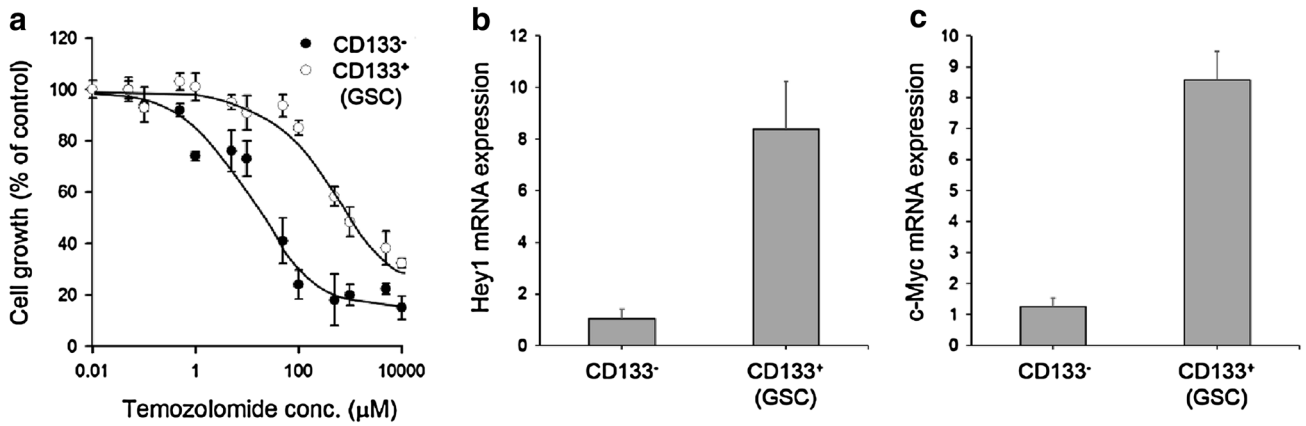

Fig. 2 Higher chemoresistance and Notch activation in GSCs. **a** Both $CD133^-$ cells and $CD133^+$ cells were treated with various concentration of Temozolomide for 48 h, growth rates were determined by MTT assay. mRNA expression of Notch target gene Hey1 (**b**) and c-Myc (**c**) in $CD133^-$ cells and $CD133^+$ cells were measured by qRT-PCR. Data shown represent the mean ± SD of three experiments

in the PEG-lipo-YO and PEG-lipo-YO-An2 was about 63.2 and 56.6 %, respectively (Table 2).

The amount of An2 attached to the liposomes was determined by the Bradford assay (Bradford 1976), and the concentration of phospholipids in liposomes was measured by phosphorus assay (Bartlett 1959). According to these measurements and the assumptions that the thickness of the lipid bilayer of the liposomes was 40 Å and the area occupied by each phospholipid was 70–75 $Å^2$ (Israelachvili and Mitchell 1975), the actual number of An2 attached to one liposome was 18–20 (Kirpotin et al. 1997).

Serum protein adsorption of PEGylated liposomes in vitro

The amount of serum protein adsorbed onto liposomal surface is related with the stability of liposomes in the blood (Cullis et al. 1998). Thus, the amount of protein (1 % BSA solution) adsorbed onto the surface of liposomes was measured by BCA protein assay. As shown in Fig. 4, the amount of protein adsorbed onto non-PEG-lipo-empty was increased significantly during incubation for 48 h, whereas PEGylated liposomes with or without YO showed only a

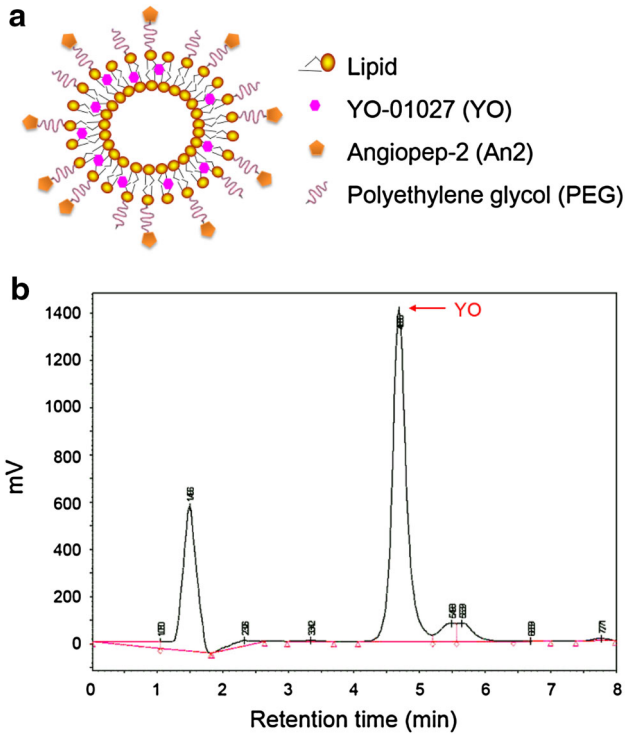

Fig. 3 Design of drug delivery system for targeting Notch activity of GSCs. **a** structure of PEG-lipo-YO-An2. **b** representative chromatogram of YO in HPLC analysis

small amount of protein adsorption. Specifically, PEGylated liposomes (PEG-lipo-empty, PEG-lipo-YO and PEG-lipo-YO-An2) adsorbed about fourfold less protein than non-PEG-lipo-empty liposomes during 48 h. The adsorption capacity of protein was significantly different in the presence and absence of PEG in liposome. This phenomenon presumably reflects the fact that PEG coating of the surface of liposomes contributes to the steric repulsion effect on serum proteins, thereby enhanced the stability of PEG-lipo-YO-An2.

Inhibition of proliferation of GSCs

The anti-proliferative effect of YO in various formulations toward GSCs was evaluated by MTT assay (Fig. 5), with PBS (control), PEG-lipo-empty, naked YO, PEG-lipo-YO and PEG-lipo-YO-An2 for 48 h. The results showed that the anti-proliferative effect of PEG-lipo-YO was greater than that of the naked drug ($P < 0.01$); this effect was further enhanced when An2-conjugated liposomes were used. Specifically, the anti-proliferative effect of PEG-lipo-YO-An2 was more than 2 times higher than that of PEG-lipo-YO ($P < 0.01$), presumably reflecting the specific targeting of LPR1 of the GSCs by An2 and enhanced stability of the PEGylated liposomes formulation. Neither PBS nor 0.1 % DMSO control or PEG-lipo-empty affected the proliferation of GSCs.

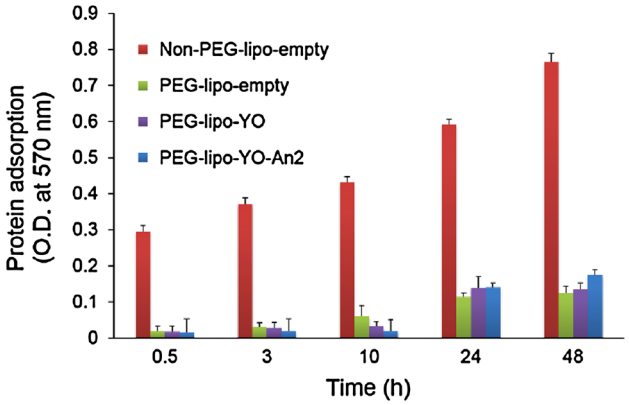

Fig. 4 Protein adsorption in 1 % BSA solution. Data shown represent the mean ± SD of four experiments

In the competition assay (Fig. 6), the anti-proliferative effect of PEG-lipo-YO-An2 was significantly decreased ($P < 0.01$) due to the competitively binding of naked An2 with LRP on GSCs, demonstrating that the anti-proliferative effect of PEG-lipo-YO-An2 could be significantly increased through LPR receptor-mediated targeting.

Tumor spheres formation assay

The stem cell property of spheroid-colony formation is considered as an indication of self-renewal ability (Takaishi et al. 2009). Figure 7 showed that untreated GSCs successfully produced spheroid colonies. Spheres treatment with naked YO, PEG-lipo-YO or PEG-lipo-YO-An2 had a suppressive effect on the formation of sphere colonies. As expected, other groups of PBS, 0.1 % DMSO and PEG-lipo-empty did not exhibit this effect. These findings

Table 2 Characterization of YO-containing liposomes

Sample	Particle size (nm)	Zeta potential (mV)	Encapsulation efficiency (%)
Non-PEG-lipo-empty	197 ± 16	−6.93 ± 2.48	–
PEG-lipo-empty	185 ± 20	−7.51 ± 7.11	–
PEG-lipo-YO	189 ± 29	−7.79 ± 4.60	63.2 ± 10.5
PEG-lipo-YO-An2	178 ± 29	−10.1 ± 3.18	56.6 ± 8.20

Data are expressed as the mean ± SD ($n = 3$)

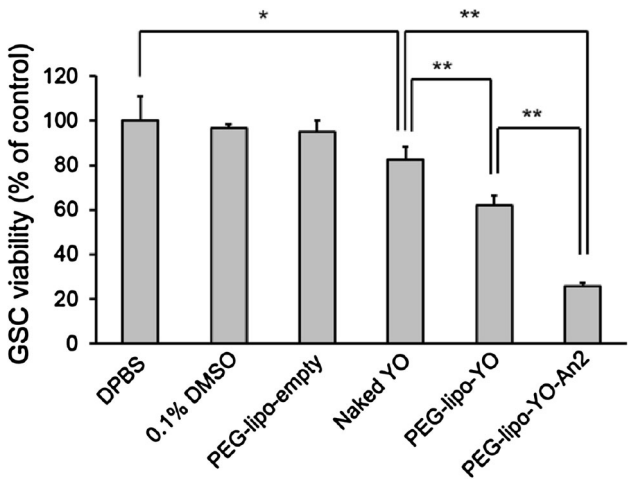

Fig. 5 In vitro cytotoxicity effect of various YO formulations towards GSCs. GSCs growth was measured by MTT assay. The data was calculated as percentage of control (DPBS) and represent the mean ± SD of six experiments (*$P < 0.05$, **$P < 0.01$)

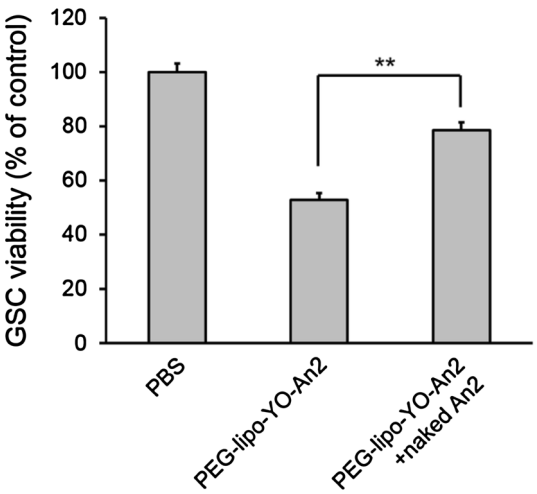

Fig. 6 Competition assay. In vitro cytotoxicity effect (%) of GSCs was decreased when GSCs was preconditioned An2 for 30 min, and followed by applying PEG-lipo-YO-An2. Data shown represent the mean ± SD of six experiments (**$P < 0.01$)

suggest that PEG-lipo-YO-An2 could greatly inhibit the ability of GSCs to form CSC-like spheroids in vitro.

Discussion

Despite recent advances in cancer therapy, the treatment of GBM remains elusive (Maher et al. 2001; Ohgaki and Kleihues 2005). GSIs are widely used to block the Notch signaling in vitro and in vivo and Notch pathway blockade by GSIs depletes $CD133^+$ glioblastoma cells and inhibits growth of tumor neurospheres and xenografts (Fan et al. 2006, 2010). Moreover, GSI-mediated inhibition of Notch signaling renders GSCs more sensitive to radiation at clinically relevant dose (Wang et al. 2010). But clinical use of GSIs, such as YO, is limited by adverse effect due to the requirement of Notch in maintaining homeostasis in most normal tissues. Besides, crossing the BBB still remains a key obstacle in delivering the most therapeutic drugs for brain disease. To overcome these limitations and enhance the anti-GSC effect of GSI, we used PEGylated liposomes as vehicles for targeted delivery of YO to block Notch signaling. On this basis, YO-loaded PEGylated liposomes were conjugated to dual-targeting ligand, An2, which targets the LRP to mediate transcytosis across the BBB and further target the GSCs. For targeting studies, we separated GSCs from the U87 MG neurosphere forming cells using an anti-CD133 antibody-based magnetic cell sorting and confirmed their properties (Fig. 1). As shown in Fig. 2, $CD133^+$ cells displayed higher Notch activity and enhanced chemoresistance. The physicochemical properties of various liposomes containing YO (Fig. 3) were also determined using particle size analyses and zeta potential measurements (Table 1). The mean diameter of liposomes for GSCs targeting was around 180 nm and zeta potential was −10.0 mV. There is a proper particle size ranging from 100 to 200 nm to improve biodistribution by accumulating in tumor tissues due to the enhanced permeability and retention (EPR) effect (Maeda et al. 2000). And negative charge on liposomes is less prone to aggregation and relatively more stable in suspension (Lian and Ho 2001). We also confirmed the stability of liposomes in the presence of serum (Fig. 4) and the amount of protein adsorption onto YO-encapsulating PEGylated liposomes was significantly decreased compared to that of non-PEGylated liposomes owing to the polymeric steric stabilizer, PEG, which results in repulsive interactions between the PEG chain and serum proteins. The actual number of An2 attached to a liposome was calculated as 18–20, and this numbers seem to be ideal as a drug targeting moiety. The anti-proliferative effect (Fig. 5) of PEG-lipo-YO-An2 showed 25.7 % of the lowest cell growth toward GSCs, compared to naked YO (80.3 %) and PEG-lipo-YO (62.0 %). Proliferation of GSCs treated with PEG-lipo-YO-An2 was significantly reduced by the addition of naked An2 in advance (Fig. 6) as LRP competitively binds with naked An2. It was also proved that liposomal delivery system showed no toxicity, as the growth inhibition of cells treated with PEG-lipo-empty was similar to the control group (Fig. 5). The above result is consistent with the results of tumor spheres formation assay (Fig. 7).

In conclusion, we developed successfully a PEG-lipo-YO-An2 formulation as a targeted delivery system for GSCs to improve therapeutic effect. PEG-lipo-YO-An2 enhanced the stability of drug delivery system, also effectively inhibited GSC proliferation and sphere

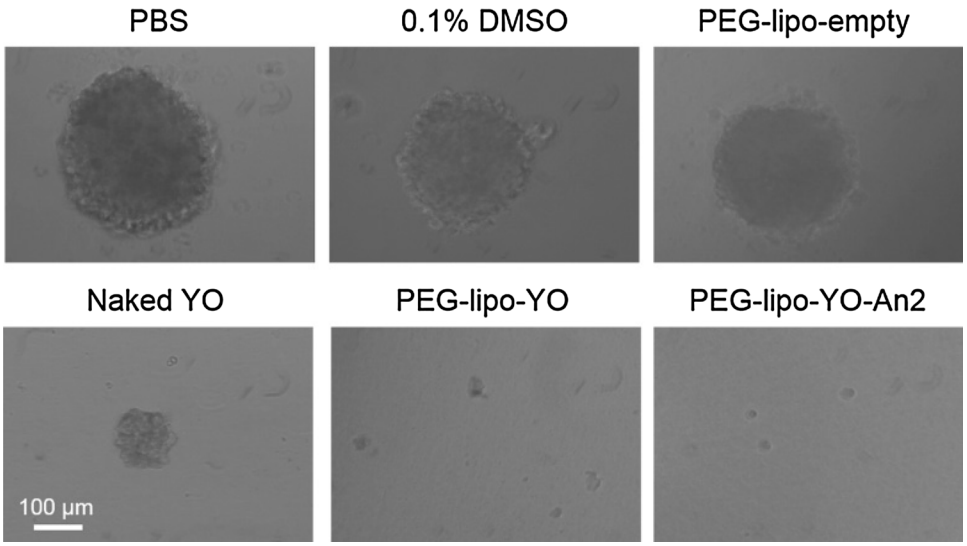

Fig. 7 Tumor spheres formation assay. Images were taken at 48 h after treating the cells with various formulations of YO (*scale bar* 100 μm)

formation. Therefore, PEG-lipo-YO-An2 is expected to be a potential agent to effectively eradicate GSCs with the in vivo anti-cancer experiment.

Acknowledgments This article does not contain any studies with human and animal subjects performed by any of the authors. All authors (S. Xuan, D. H. Shin and J. S. Kim) declare that they have no conflict of interest. This work was supported by the National Research Foundation of Korea (NRF) grant funded by the Korea government (MSIP) (no. 2011-0030074) and by Basic Science Research Program through the National Research Foundation of Korea (NRF) funded by the Ministry of Science, ICT and Future Planning (2014R1A2A2A01004353).

References

Akbarzadeh A, Rezaei-Sadabady R, Davaran S, Joo SW, Zarghami N, Hanifehpour Y, Samiei M, Kouhi M, Nejati-Koshki K (2013) Liposome: classification, preparation, and applications. Nanoscale Res Lett 8:102

Bartlett GR (1959) Phosphorus assay in column chromatography. J Biol Chem 234:466–468

Bradford MM (1976) A rapid and sensitive method for the quantitation of microgram quantities of protein utilizing the principle of protein-dye binding. Anal Biochem 72:248–254

Chow TH, Lin YY, Hwang JJ, Wang HE, Tseng YL, Wang SJ, Liu RS, Lin WJ, Yang CS, Ting G (2009) Improvement of biodistribution and therapeutic index via increase of polyethylene glycol on drug-carrying liposomes in an HT-29/luc xenografted mouse model. Anticancer Res 29:2111–2120

Cullis PR, Chonn A, Semple SC (1998) Interactions of liposomes and lipid-based carrier systems with blood proteins: relation to clearance behaviour in vivo. Adv Drug Deliv Rev 32:3–17

Demeule M, Currie JC, Bertrand Y, Che C, Nguyen T, Regina A, Gabathuler R, Castaigne JP, Beliveau R (2008) Involvement of the low-density lipoprotein receptor-related protein in the transcytosis of the brain delivery vector angiopep-2. J Neurochem 106:1534–1544

Ehebauer M, Hayward P, Martinez-Arias A (2006) Notch signaling pathway. Sci STKE 364(2006):7

Fan X, Matsui W, Khaki L, Stearns D, Chun J, Li YM, Eberhart CG (2006) Notch pathway inhibition depletes stem-like cells and blocks engraftment in embryonal brain tumors. Cancer Res 66:7445–7452

Fan X, Khaki L, Zhu TS, Soules ME, Talsma CE, Gul N, Koh C, Zhang J, Li YM, Maciaczyk J, Nikkhah G, Dimeco F, Piccirillo S, Vescovi AL, Eberhart CG (2010) NOTCH pathway blockade depletes CD133-positive glioblastoma cells and inhibits growth of tumor neurospheres and xenografts. Stem Cells 28:5–16

Galli R, Binda E, Orfanelli U, Cipelletti B, Gritti A, De Vitis S, Fiocco R, Foroni C, Dimeco F, Vescovi A (2004) Isolation and characterization of tumorigenic, stem-like neural precursors from human glioblastoma. Cancer Res 64:7011–7021

Garner JM, Fan M, Yang CH, Du Z, Sims M, Davidoff AM, Pfeffer LM (2013) Constitutive activation of signal transducer and activator of transcription 3 (STAT3) and nuclear factor kappaB signaling in glioblastoma cancer stem cells regulates the Notch pathway. J Biol Chem 288:26167–26176

Gref R, Luck M, Quellec P, Marchand M, Dellacherie E, Harnisch S, Blunk T, Muller RH (2000) 'Stealth' corona-core nanoparticles surface modified by polyethylene glycol (PEG): influences of the corona (PEG chain length and surface density) and of the core composition on phagocytic uptake and plasma protein adsorption. Colloids Surf B Biointerfaces 18:301–313

Guichet PO, Guelfi S, Teigell M, Hoppe L, Bakalara N, Bauchet L, Duffau H, Lamszus K, Rothhut B, Hugnot JP (2014). Notch1 stimulation induces a vascularization switch with pericyte-like cell differentiation of glioblastoma stem cells. Stem Cells [in press]

Hemmati HD, Nakano I, Lazareff JA, Masterman-Smith M, Geschwind DH, Bronner-Fraser M, Kornblum HI (2003) Cancerous stem cells can arise from pediatric brain tumors. Proc Natl Acad Sci U S A 100:15178–15183

Hovinga KE, Shimizu F, Wang R, Panagiotakos G, Van Der Heijden M, Moayedpardazi H, Correia AS, Soulet D, Major T, Menon J, Tabar V (2010) Inhibition of notch signaling in glioblastoma targets cancer stem cells via an endothelial cell intermediate. Stem Cells 28:1019–1029

Hu YY, Zheng MH, Cheng G, Li L, Liang L, Gao F, Wei YN, Fu LA, Han H (2011) Notch signaling contributes to the maintenance of both normal neural stem cells and patient-derived glioma stem cells. BMC Cancer 11:82

Hu YY, Fu LA, Li SZ, Chen Y, Li JC, Han J, Liang L, Li L, Ji CC, Zheng MH, Han H (2014) Hif-1alpha and Hif-2alpha differentially regulate Notch signaling through competitive interaction

with the intracellular domain of Notch receptors in glioma stem cells. Cancer Lett 349:67–76

Huang S, Li J, Han L, Liu S, Ma H, Huang R, Jiang C (2011) Dual targeting effect of Angiopep-2-modified, DNA-loaded nanoparticles for glioma. Biomaterials 32:6832–6838

Iso T, Kedes L, Hamamori Y (2003) HES and HERP families: multiple effectors of the Notch signaling pathway. J Cell Physiol 194:237–255

Israelachvili JN, Mitchell DJ (1975) A model for the packing of lipids in bilayer membranes. Biochim Biophys Acta 389:13–19

Kirpotin D, Park JW, Hong K, Zalipsky S, Li WL, Carter P, Benz CC, Papahadjopoulos D (1997) Sterically stabilized anti-HER2 immunoliposomes: design and targeting to human breast cancer cells in vitro. Biochemistry 36:66–75

Li JL, Sainson RC, Shi W, Leek R, Harrington LS, Preusser M, Biswas S, Turley H, Heikamp E, Hainfellner JA, Harris AL (2007) Delta-like 4 Notch ligand regulates tumor angiogenesis, improves tumor vascular function, and promotes tumor growth in vivo. Cancer Res 67:11244–11253

Lian T, Ho RJ (2001) Trends and developments in liposome drug delivery systems. J Pharm Sci 90:667–680

Lopes MB, Bogaev CA, Gonias SL, VandenBerg SR (1994) Expression of alpha 2-macroglobulin receptor/low density lipoprotein receptor-related protein is increased in reactive and neoplastic glial cells. FEBS Lett 338:301–305

Louvi A, Artavanis-Tsakonas S (2006) Notch signalling in vertebrate neural development. Nat Rev Neurosci 7:93–102

Maeda H, Wu J, Sawa T, Matsumura Y, Hori K (2000) Tumor vascular permeability and the EPR effect in macromolecular therapeutics: a review. J Control Release 65:271–284

Maher EA, Furnari FB, Bachoo RM, Rowitch DH, Louis DN, Cavenee WK, DePinho RA (2001) Malignant glioma: genetics and biology of a grave matter. Genes Dev 15:1311–1333

Mamaeva V, Rosenholm JM, Bate-Eya LT, Bergman L, Peuhu E, Duchanoy A, Fortelius LE, Landor S, Toivola DM, Linden M, Sahlgren C (2011) Mesoporous silica nanoparticles as drug delivery systems for targeted inhibition of Notch signaling in cancer. Mol Ther 19:1538–1546

Miraglia S, Godfrey W, Yin AH, Atkins K, Warnke R, Holden JT, Bray RA, Waller EK, Buck DW (1997) A novel five-transmembrane hematopoietic stem cell antigen: isolation, characterization, and molecular cloning. Blood 90:5013–5021

Moellering RE, Cornejo M, Davis TN, Del Bianco C, Aster JC, Blacklow SC, Kung AL, Gilliland DG, Verdine GL, Bradner JE (2009) Direct inhibition of the NOTCH transcription factor complex. Nature 462:182–188

Ohgaki H, Kleihues P (2005) Population-based studies on incidence, survival rates, and genetic alterations in astrocytic and oligodendroglial gliomas. J Neuropathol Exp Neurol 64:479–489

Pardridge WM (1999) Blood-brain barrier biology and methodology. J Neurovirol 5:556–569

Pardridge WM (2005) The blood-brain barrier: bottleneck in brain drug development. NeuroRx 2:3–14

Pardridge WM (2007) Drug targeting to the brain. Pharm Res 24:1733–1744

Park DM, Rich JN (2009) Biology of glioma cancer stem cells. Mol Cells 28:7–12

Purow B (2012) Notch inhibition as a promising new approach to cancer therapy. Adv Exp Med Biol 727:305–319

Radtke F, Raj K (2003) The role of Notch in tumorigenesis: oncogene or tumour suppressor? Nat Rev Cancer 3:756–767

Ren J, Shen S, Wang D, Xi Z, Guo L, Pang Z, Qian Y, Sun X, Jiang X (2012) The targeted delivery of anticancer drugs to brain glioma by PEGylated oxidized multi-walled carbon nanotubes modified with angiopep-2. Biomaterials 33:3324–3333

Reya T, Morrison SJ, Clarke MF, Weissman IL (2001) Stem cells, cancer, and cancer stem cells. Nature 414:105–111

Ridgway J, Zhang G, Wu Y, Stawicki S, Liang WC, Chanthery Y, Kowalski J, Watts RJ, Callahan C, Kasman I, Singh M, Chien M, Tan C, Hongo JA, de Sauvage F, Plowman G, Yan M (2006) Inhibition of Dll4 signalling inhibits tumour growth by deregulating angiogenesis. Nature 444:1083–1087

Rizzo P, Osipo C, Foreman K, Golde T, Osborne B, Miele L (2008) Rational targeting of Notch signaling in cancer. Oncogene 27:5124–5131

Sahebjam S, Bedard PL, Castonguay V, Chen Z, Reedijk M, Liu G, Cohen B, Zhang WJ, Clarke B, Zhang T, Kamel-Reid S, Chen H, Ivy SP, Razak AR, Oza AM, Chen EX, Hirte HW, McGarrity A, Wang L, Siu LL, Hotte SJ (2013) A phase I study of the combination of ro4929097 and cediranib in patients with advanced solid tumours (PJC-004/NCI 8503). Br J Cancer 109:943–949

Saito N, Fu J, Zheng S, Yao J, Wang S, Liu DD, Yuan Y, Sulman EP, Lang FF, Colman H, Verhaak RG, Yung WK, Koul D (2014) A high Notch pathway activation predicts response to gamma secretase inhibitors in proneural subtype of glioma tumor-initiating cells. Stem Cells 32:301–312

Sanai N, Alvarez-Buylla A, Berger MS (2005) Neural stem cells and the origin of gliomas. N Engl J Med 353:811–822

Schott AF, Landis MD, Dontu G, Griffith KA, Layman RM, Krop I, Paskett LA, Wong H, Dobrolecki LE, Lewis MT, Froehlich AM, Paranilam J, Hayes DF, Wicha MS, Chang JC (2013) Preclinical and clinical studies of gamma secretase inhibitors with docetaxel on human breast tumors. Clin Cancer Res 19:1512–1524

Shao K, Wu J, Chen Z, Huang S, Li J, Ye L, Lou J, Zhu L, Jiang C (2012) A brain-vectored angiopep-2 based polymeric micelles for the treatment of intracranial fungal infection. Biomaterials 33:6898–6907

Shi S, Han L, Gong T, Zhang Z, Sun X (2013) Systemic delivery of microRNA-34a for cancer stem cell therapy. Angew Chem Int Ed Engl 52:3901–3905

Shih AH, Holland EC (2006) Notch signaling enhances nestin expression in gliomas. Neoplasia 8:1072–1082

Singh SK, Clarke ID, Terasaki M, Bonn VE, Hawkins C, Squire J, Dirks PB (2003) Identification of a cancer stem cell in human brain tumors. Cancer Res 63:5821–5828

Singh SK, Hawkins C, Clarke ID, Squire JA, Bayani J, Hide T, Henkelman RM, Cusimano MD, Dirks PB (2004) Identification of human brain tumour initiating cells. Nature 432:396–401

Sun X, Pang Z, Ye H, Qiu B, Guo L, Li J, Ren J, Qian Y, Zhang Q, Chen J, Jiang X (2012) Co-delivery of pEGFP-hTRAIL and paclitaxel to brain glioma mediated by an angiopep-conjugated liposome. Biomaterials 33:916–924

Takaishi S, Okumura T, Tu S, Wang SS, Shibata W, Vigneshwaran R, Gordon SA, Shimada Y, Wang TC (2009) Identification of gastric cancer stem cells using the cell surface marker CD44. Stem Cells 27:1006–1020

Telerman A, Amson R (2009) The molecular programme of tumour reversion: the steps beyond malignant transformation. Nat Rev Cancer 9:206–216

van Es JH, van Gijn ME, Riccio O, van den Born M, Vooijs M, Begthel H, Cozijnsen M, Robine S, Winton DJ, Radtke F, Clevers H (2005) Notch/gamma-secretase inhibition turns proliferative cells in intestinal crypts and adenomas into goblet cells. Nature 435:959–963

Wang L, Rahn JJ, Lun X, Sun B, Kelly JJ, Weiss S, Robbins SM, Forsyth PA, Senger DL (2008) Gamma-secretase represents a therapeutic target for the treatment of invasive glioma mediated by the p75 neurotrophin receptor. PLoS Biol 6:e289

Wang J, Wakeman TP, Lathia JD, Hjelmeland AB, Wang XF, White RR, Rich JN, Sullenger BA (2010) Notch promotes radioresistance of glioma stem cells. Stem Cells 28:17–28

Wen PY, Kesari S (2008) Malignant gliomas in adults. N Engl J Med 359:492–507

Wong GT, Manfra D, Poulet FM, Zhang Q, Josien H, Bara T, Engstrom L, Pinzon-Ortiz M, Fine JS, Lee HJ, Zhang L, Higgins GA, Parker EM (2004) Chronic treatment with the gamma-secretase inhibitor LY-411,575 inhibits beta-amyloid peptide production and alters lymphopoiesis and intestinal cell differentiation. J Biol Chem 279:12876–12882

Wu Y, Cain-Hom C, Choy L, Hagenbeek TJ, de Leon GP, Chen Y, Finkle D, Venook R, Wu X, Ridgway J, Schahin-Reed D, Dow GJ, Shelton A, Stawicki S, Watts RJ, Zhang J, Choy R, Howard P, Kadyk L, Yan M, Zha J, Callahan CA, Hymowitz SG, Siebel CW (2010) Therapeutic antibody targeting of individual Notch receptors. Nature 464:1052–1057

Xin H, Jiang X, Gu J, Sha X, Chen L, Law K, Chen Y, Wang X, Jiang Y, Fang X (2011) Angiopep-conjugated poly(ethylene glycol)-co-poly(epsilon-caprolactone) nanoparticles as dual-targeting drug delivery system for brain glioma. Biomaterials 32: 4293–4305

Xin H, Sha X, Jiang X, Chen L, Law K, Gu J, Chen Y, Wang X, Fang X (2012a) The brain targeting mechanism of Angiopep-conjugated poly(ethylene glycol)-co-poly(epsilon-caprolactone) nanoparticles. Biomaterials 33:1673–1681

Xin H, Sha X, Jiang X, Zhang W, Chen L, Fang X (2012b) Anti-glioblastoma efficacy and safety of paclitaxel-loading Angiopep-conjugated dual targeting PEG-PCL nanoparticles. Biomaterials 33:8167–8176

Yan M, Callahan CA, Beyer JC, Allamneni KP, Zhang G, Ridgway JB, Niessen K, Plowman GD (2010) Chronic DLL4 blockade induces vascular neoplasms. Nature 463:E6–E7

Yu Y, Flint A, Dvorin EL, Bischoff J (2002) AC133-2, a novel isoform of human AC133 stem cell antigen. J Biol Chem 277:20711–20716

Yuan X, Curtin J, Xiong Y, Liu G, Waschsmann-Hogiu S, Farkas DL, Black KL, Yu JS (2004) Isolation of cancer stem cells from adult glioblastoma multiforme. Oncogene 23:9392–9400

Zhang XP, Zheng G, Zou L, Liu HL, Hou LH, Zhou P, Yin DD, Zheng QJ, Liang L, Zhang SZ, Feng L, Yao LB, Yang AG, Han H, Chen JY (2008) Notch activation promotes cell proliferation and the formation of neural stem cell-like colonies in human glioma cells. Mol Cell Biochem 307:101–108

Zhang GS, Tian Y, Huang JY, Tao RR, Liao MH, Lu YM, Ye WF, Wang R, Fukunaga K, Lou YJ, Han F (2013) The gamma-secretase blocker DAPT reduces the permeability of the blood-brain barrier by decreasing the ubiquitination and degradation of occludin during permanent brain ischemia. CNS Neurosci Ther 19:53–60

Zhu X, Bidlingmaier S, Hashizume R, James CD, Berger MS, Liu B (2010) Identification of internalizing human single-chain antibodies targeting brain tumor sphere cells. Mol Cancer Ther 9:2131–2141